Electronic structure of the 4H polytype of diamond

1996 J. Phys.: Condens. Matter 8 5801

(http://iopscience.iop.org/0953-8984/8/31/013)

J. Phys.: Condens. Matter **8** (1996) 5801–5809. Printed in the UK

Electronic structure of the 4H polytype of diamond

A K Sharma†, H G Salunke‡, G P Das‡, P Ayyub† and M S Multani†

† Materials Research Group, Tata Institute of Fundamental Research, Homi Bhabha Road, Bombay 400 005, India

‡ Solid State Physics Division, Bhabha Atomic Research Centre, Bombay 400 085, India

Received 29 January 1996, in final form 9 April 1996

Abstract. We report the core-level x-ray photoelectron spectrum (XPS) of 4H diamond—a higher polytype of the well-studied cubic diamond. Diamond polytype films were synthesized by laser-induced reactive quenching at a liquid–solid interface, and characterized by transmission electron micro-diffraction. Electronic energy bands and densities of states, calculated using the local-density-based tight-binding linear muffin-tin orbital method, have been used to interpret the XPS data.

1. Introduction

The advent of low-pressure routes for the synthesis of diamond has resulted in a plethora of scientific and technical literature that focus on the nucleation mechanism, doping effects, and possible applications in electronics, and as optical windows, wear-resistant coatings, etc [1–6]. Diamond occurs most frequently, and has been best studied, in the cubic ('3C') structure. However, several polytypic structures are predicted for diamond [7] (of which a few have actually been observed), and these are analogous to the SiC polytypes [8]. A number of compounds with close-packed, layered structures exhibit polymorphism along a single crystallographic direction (along which the layers are stacked). The 'in-plane' unit-cell parameters of such *polytypes* are identical (in principle), but those along the stacking direction differ—being integral multiples of the unit-layer separation.

The lonsdaleite polytype of diamond with hexagonal ('2H') structure [9] is energetically less favourable, and is therefore observed less frequently than the cubic form. Both of the structures can be described in terms of identical puckered layers of sp^3-bonded six-membered rings of carbon atoms. They differ only in the manner in which these layers are stacked along the *c*-direction—either in the 'chair' (3C) or in the 'boat' (2H) conformation. The stacking sequences in the higher diamond polytypes (4H, 6H, 8H, etc) incorporate the boat as well as the chair units [10]. Though the 4H and 6H polytypes have been observed experimentally [11, 12], little is known of their cohesive, electronic and optical properties, and their stabilities relative to the parent structures. Such investigations should prove very interesting—in view of the excellent combination of properties exhibited by cubic diamond.

Here we report first-principles electronic structure calculations on the 4H polytype of diamond and its parent structures (3C and 2H) under the local density approximation (LDA) using the tight-binding linear muffin-tin orbital (TB-LMTO) method [13, 14] within the atomic-sphere approximation (ASA) [15]. The higher polytypes compete with each other with extremely close ground-state energies that lie *between* those of the 3C and 2H structures. Using the Andersen force theorem [16] to determine the stability sequence of

0953-8984/96/315801+09$19.50

these structures, the 4H polytype was earlier found to be energetically most favourable, followed by 6H and 8H respectively [17]. Of course, these higher polytypes are metastable with respect to 3C and therefore require non-equilibrium growth conditions. Attempts to selectively grow higher diamond polytypes may not be successful unless one achieves very precise control over the relevant experimental parameters.

We have recently indicated the possibility of synthesizing higher polytypes of diamond [12] using pulsed laser-induced reactive quenching at the interface of a judiciously chosen organic liquid and a solid substrate. The molecules of the organic compounds used (cyclohexane and decalin) consist of the same chair and boat units that are the building blocks of cubic and hexagonal diamond. A detailed structural analysis of the diamond films prepared as above using transmission electron diffraction (TED), showed the 4H polytype to be predominant [18]. Here, we present the C 1s energy-loss structure from x-ray photoelectron spectroscopy (XPS) measurements on such diamond films and attempt to analyse it on the basis of the electron energy bands and l-projected densities of states (DOS) calculated for this structure.

2. Synthesis and characterization of 4H diamond

The diamond polytype films were deposited by pulsed laser-induced reactive quenching. An organic liquid, decalin (which has a mixture of six-membered carbon rings in the chair and boat conformations), was supported on a polycrystalline tungsten substrate. A pulsed excimer laser beam (pulse width $\cong$ 20 ns, energy density $\cong$ 3.5 J cm^{-2}) was focused on the liquid–solid interface and several laser pulses were shot at a single point. A large area of the surface ($\approx$1 cm^2) was scanned in this way. Further details of the synthesis technique are described elsewhere [12, 18].

Samples for transmission electron microscopy (TEM) studies were prepared with the help of a Gatan ion mill. The specimens were thinned mainly from the substrate side and slightly from the film side to clean the surface. They were then examined in a Jeol 2000FX electron microscope. The TEM was operated in a micro-diffraction mode with an incident electron beam diameter of $\approx$2 nm, and TED patterns were recorded from individual crystallites.

Figure 1 shows an electron micro-diffraction pattern from one of the crystallites in the diamond polytype film. The pattern shows the $(01\bar{1}0)$ and the $(10\bar{1}5)$ reflections of the 4H diamond polytype, the corresponding d-spacings being 2.190 Å and 1.315 Å, respectively. The measured values of the lattice parameters ($a = 2.522$ Å, $c = 8.234$ Å) are in excellent agreement with the values ($a = 2.5221$ Å, $c = 8.2371$ Å) predicted by Holcombe *et al* (see [7]). The angle between these two directions ($(01\bar{1}0)$ and $(10\bar{1}5)$) was calculated taking the measured c/a-ratio. The experimental value of this angle ($72.5 \pm 1.0^\circ$) matches well with the calculated value of 72° (data from ASTM card No 26-1078). Additional details of the TEM studies of 4H diamond can be found in [18].

3. Band structures of 3C and 4H diamond

Electron structure calculations have been performed using the self-consistent TB-LMTO-ASA method with the 'frozen-core' approximation and von Barth–Hedin parametrization [19] of the exchange–correlation potential. In this method, the crystal is divided into space-filling and therefore slightly overlapping atomic spheres centred on each of the atomic sites. Since the diamond polytypes under consideration are relatively open structures (low packing

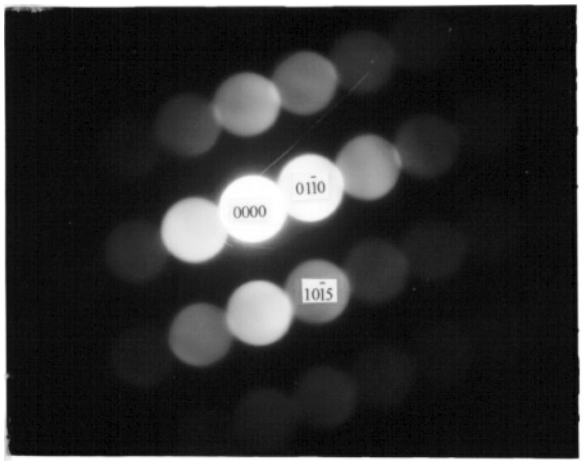

Figure 1. The transmission electron micro-diffraction pattern from a crystallite in a 4H diamond film. The (01$\bar{1}$0) and the (10$\bar{1}$5) reflections are indicated.

fraction), it is essential to introduce so-called empty spheres at appropriate positions, so that the sphere overlaps are within the allowable limits of the ASA [14].

Table 1. Input parameters for the self-consistent LMTO-ASA calculations for 3C, 2H and 4H diamond polytypes. C and E denote carbon spheres and empty spheres, respectively. The atomic positions (from [30]) refer to the space group D^4_{6h} for 4H and D^5_{3d} for 3C diamond†; and z is the internal position parameter. W is the average Wigner–Seitz sphere radius (=1.659 39 au) and the cell parameter $a = 2.52$ Å.

		Chair units				Boat units					
		Atomic positions		Atomic radii		Atomic positions			Atomic radii		
	c/a	C	E	R(C)/W	R(E)/W	C	E_1	E_2	R(C)/W	$R(E_1)/W$	$R(E_2)/W$
3C	2.449 49	6c ($z = 9/24$)	6c ($z = 3/24$)	1.0	1.0	—	—	—	—	—	—
2H	1.632 99	—	—	—	—	4f ($z = 1/16$)	2b	2d	1.0	1.187	0.690
4H	3.265 98	4e ($z = 3/52$)	4f ($z = 17/32$)	1.0	1.0	4f ($z = 5/32$)	2d	2b	1.0	1.187	0.690

† The positions of the carbon atoms and the empty spheres in cubic diamond (O^7_h) are 8a and 8b, respectively. However, cubic diamond can be viewed along the ⟨111⟩ direction, resulting in a hexagonal unit cell (D^5_{3d}) with $a = 2.52$ Å and $c/a = 2.449$. The 8a and 8b positions of the cubic unit cell are equivalent to the 6c positions of the hexagonal cell.

Cubic (3C) diamond, when viewed along the ⟨111⟩ direction, has six carbon atoms per unit cell and an ABC/ABC/$\cdots$ type of stacking sequence, while hexagonal (2H) diamond has four carbon atoms per unit cell and an AB/AB/$\cdots$ stacking [8]. In this notation, 'A', 'B', and 'C' each represent a pair of atomic layers stacked on top of each other, with the successive pairs being displaced sideways [10]. The 4H structure has an ABCB/ABCB/$\cdots$ stacking, and can be visualized as consisting of alternate chair and boat units (figure 2). In order to ensure artificial close packing of this type of structure, we assume each chair unit to consist of two carbon atoms (one double layer) and two empty spheres of the same

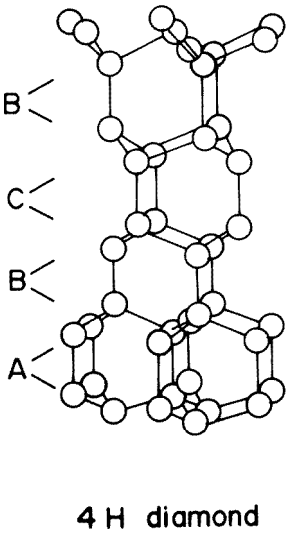

Figure 2. The crystal structure of the 4H polytype of diamond showing one repeat unit of the ABCB/ABCB$\cdots$ stacking. The stacking sequence in 'normal', cubic (3C) diamond is ABC/ABC$\cdots$, which can be visualized by simply removing the uppermost (B) bilayer in this figure.

radius, while each boat unit is assumed to consist of two carbon atoms and two empty spheres of *different* radii. The atomic positions and the sphere radii are given in table 1. We have used s, p and d partial waves for solutions within the carbon spheres, and s and p partial-wave solutions within the empty spheres. The d partial waves in carbon have been 'downfolded' [20]. We have also included the so-called 'combined correction' term [15] in our calculation.

Table 2. Energy values corresponding to peaks in the density of states in the occupied and unoccupied energy bands of 3C diamond. The transition energies (ΔE) are also shown.

s DOS	p DOS	ΔE(s $\rightarrow$ p) (eV)	ΔE(p $\rightarrow$ s) (eV)
Occupied states (eV)		19.5	10.5
−17.0	−11.5	22.0	13.5
−14.0	−6.5	24.5	14.0
−11.5	−3.5	25.0	17.0
Unoccupied states (eV)		26.5	18.5
7.0	8.0	27.5	21.5
10.5	10.5	29.0	22.0
15.0	15.0	32.0	26.5

The l-projected DOS for the 3C and 4H polytypes of diamond are presented in figure 3. All allowed interband transitions satisfying the dipole-selection rules ($\Delta l = \pm 1$) can be obtained from the l-projected DOS. The energy values pertaining to the peaks appearing in the l-projected DOS for the occupied and the unoccupied states in 3C diamond have been tabulated and the corresponding transition energies indicated in table 2. The prominent features in the s DOS and the p DOS for 4H diamond, together with the expected transitions, are also tabulated (table 3). In view of the approximations involved in the linearized band

Table 3. Energy values corresponding to peaks in the density of states in the occupied and unoccupied energy bands of 4H diamond. The transition energies (ΔE) are also shown.

s DOS	p DOS	ΔE(s → p) (eV)	ΔE(p → s) (eV)
Occupied states (eV)		23.0	10.5
−16.5	−6.5	24.5	12.0
	−4.0	26.5	13.0
Unoccupied states (eV)		28.0	14.5
6.5	6.5	30.5	17.5
8.0	8.0	32.5	19.0
13.5	10.0		20.0
15.0	11.5		21.5
	14.0		26.5
	16.0		

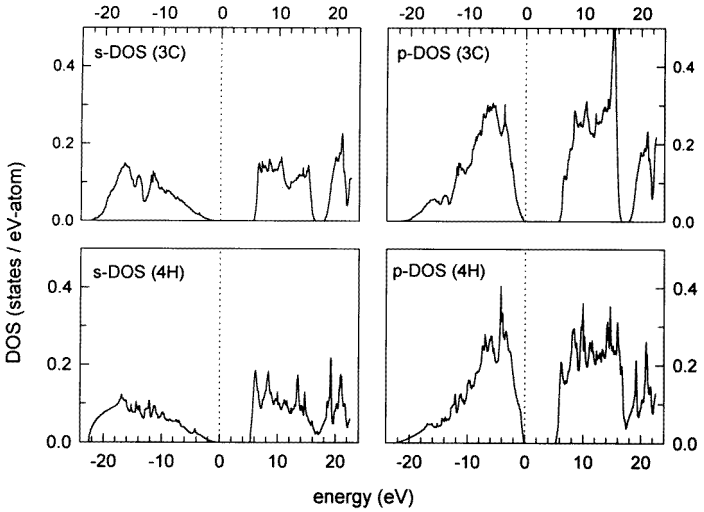

Figure 3. The calculated densities of states for 3C and 4H diamond. The dotted lines indicate the positions of the corresponding Fermi energies.

calculation method used here, we have ignored the higher-energy peaks in the unoccupied part of the DOS.

Strong contributions are expected in optical spectra from those $\boldsymbol{k}$-points for which $\boldsymbol{\nabla}_k E_C(\boldsymbol{k}) = 0$, and $\boldsymbol{\nabla}_k E_V(\boldsymbol{k}) = 0$. Critical points of this type occur only at high-symmetry points in the Brillouin zone. Most of the 'expected' transitions (table 2) had not been observed in the electron energy-loss spectra (EELS) or C 1s loss structure (in XPS) reported earlier for cubic diamond [21–23]. It is clear from the band structures for both 3C and 4H diamond (figure 4) that most of these transitions are indirect. An important exception is the transition for 3C (indicated in figure 4(a)) at about 14 eV, which lies along the M point where there are flat bands in both the bonding (at ≈ -6.5 eV on the p DOS) and the antibonding (lowest conduction band) states. Indeed, an interband transition occurring between 14 and 17 eV has been observed for cubic diamond [22, 23], along with the surface and bulk plasmon peaks at around 23 and 35 eV, respectively. Observation of indirect transitions in XPS is not ruled out [24] owing to the fact that the

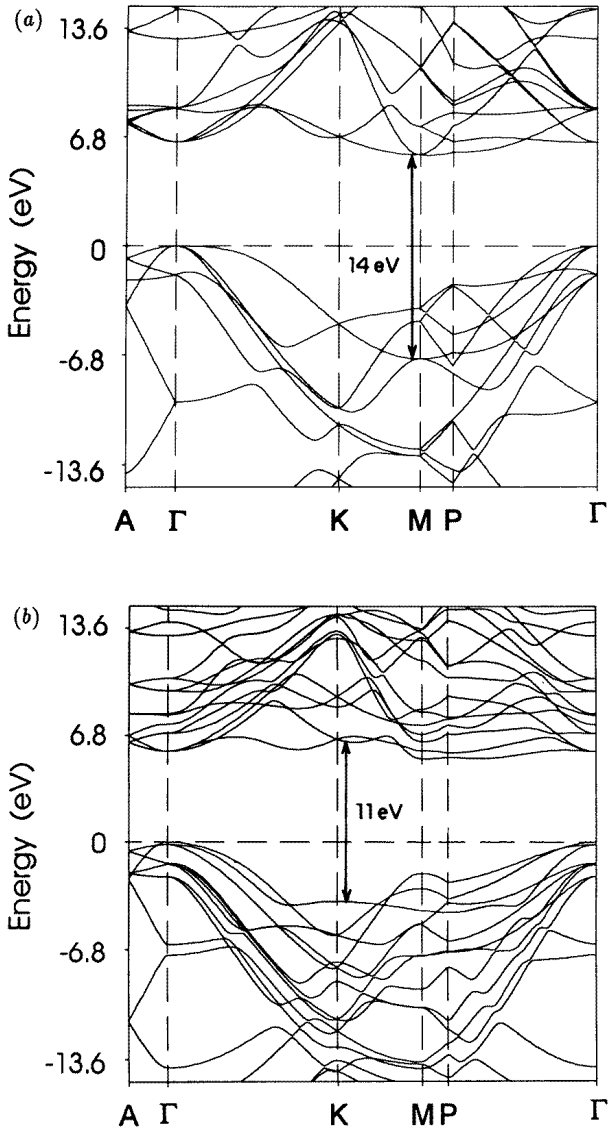

Figure 4. Electronic band structures of (*a*) 3C and (*b*) 4H diamond. The energy values corresponding to the most prominent transitions are indicated.

wave vector corresponding to the primary beam (∼1 keV) needs to be included in the wave-vector-conservation equation, unlike in ultraviolet photoelectron spectroscopy. Such indirect transitions can be induced in a number of ways—for example, by interaction with phonons or by the introduction of atomic disorder. In a previous study of diamond using EELS with a primary beam energy of 300 eV, most of the transitions predicted by us for cubic diamond had been observed in the second-derivative spectra [25]. To the best of our knowledge, that is the only study of cubic diamond which shows the relatively large number of interband transitions predicted by our calculations.

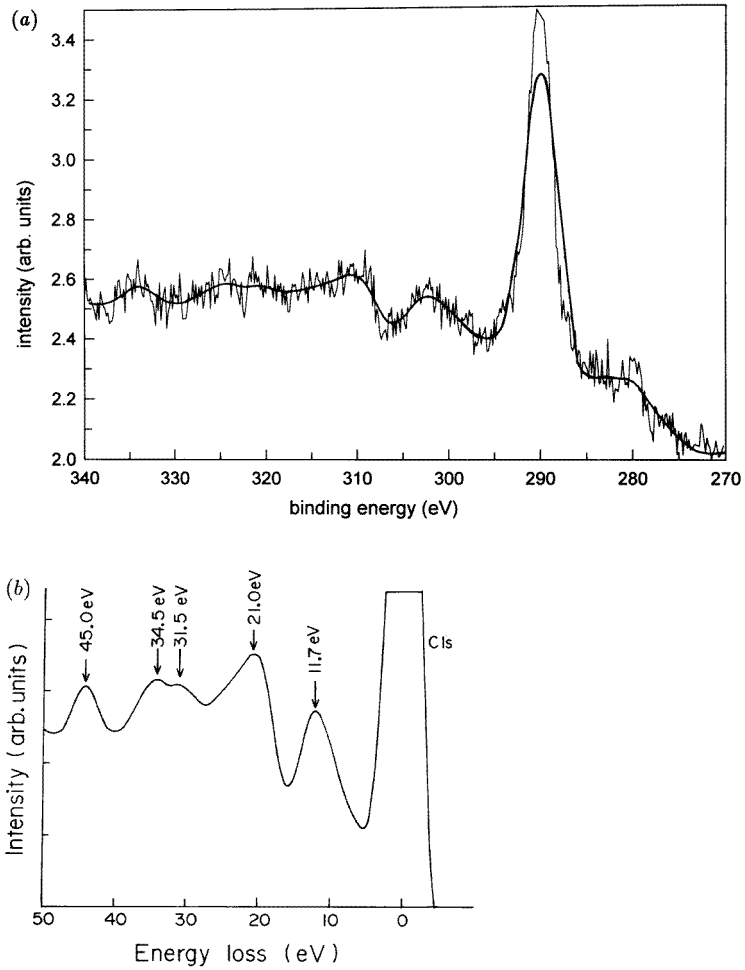

Figure 5. (*a*) The x-ray photoelectron spectrum (C 1s) recorded for 4H diamond. Both the raw data and the envelope of the best fit are shown. (*b*) The fitted XPS data magnified and replotted in terms of energy loss with respect to the C 1s peak. The positions of the loss peaks are indicated in the figure.

4. XPS study of 4H diamond

The C 1s XPS spectra were recorded on a VSW Scientific Instruments spectrometer, with the Al Kα (1.4866 keV) line as the excitation source. The base vacuum was better than 10^{-9} Torr. The net resolution achievable with the concentric hemispherical analyser was $\approx$0.8 eV. The Ag $3d_{5/2}$ line was used as an external standard. A total of 10 scans were recorded to improve the signal-to-noise ratio. The spectra were smoothed using a fast-Fourier-transform process and the peaks fitted with a Gaussian–Lorentzian combination. The raw data as well as the fitted curve (envelope) are shown in figure 5(*a*), while the fitted spectrum is magnified and replotted in figure 5(*b*) with the C 1s peak position as the origin, in order to indicate the energy loss suffered by the C 1s electrons in undergoing inelastic collisions with the valence electrons of the constituent atoms. In the past, the XPS

loss structure has been used extensively to characterize materials through plasmon loss, interband and intraband transitions [21, 26].

In our diamond polytype films (which are predominantly of 4H diamond), the strong interband transition observed at 11.7 eV (figure 5(*b*)) is quite close to the transitions estimated above for 4H diamond (table 3). This peak observed in the XPS loss structure of 4H diamond is a prominent feature, as opposed to the small hump or shoulder observed for cubic diamond at around 13–17 eV by a number of workers [22, 23]. In the band structure of 4H diamond (figure 4(*b*)), we observe flat bands around the K point in both the occupied as well as the unoccupied parts of the energy spectra, which are expected to result in a strong XPS loss peak at ≈11 eV. Interestingly, this unique feature is not observed in the band structure of any other diamond polytype (3C, 2H, 6H, and 8H), though all of them have their largest direct gap in this direction. The strong interband transition at ≈11 eV, therefore, appears to characterize the 4H phase.

The other features in the XPS loss spectrum—namely, the peaks at 21 and 34.5 eV—can be ascribed respectively to the surface and bulk plasmon modes of diamond. These are expected to be the same in all of the diamond phases since they depend only on the valence electron density. A small hump at 31.5 eV may be assigned to the bulk plasmon loss of amorphous carbon [21, 27]. The coexistence of a small amount of sp^2-bonded phase (from amorphous carbon) is typical of diamond films grown by CVD and other techniques—as observed by laser Raman spectroscopy [5, 28]. The feature at ≈45 eV can be assigned to the bulk plasmon loss at ≈34 eV followed (or preceded) by an interband transition of ≈11 eV. A similar type of combined transition has previously been observed for the C 1s loss spectrum of cubic diamond [29].

5. Conclusion

We have studied the electronic band structure and the interband transitions for the 4H polytype of diamond, using self-consistent LDA calculations. The densities of states and the energy bands for this polytype are compared with those of conventional cubic diamond. These results, in conjunction with our XPS energy-loss data, suggest that a prominent interband transition at ≈11 eV is a signature of 4H diamond. A detailed study of the nature of the bonding, cohesive properties and charge densities in the different members of the diamond family will be reported separately.

Acknowledgments

It is a pleasure to thank Dr K P Adhi, Dr D S Joag and Professor S B Ogale for allowing us to use their laser deposition facilities at the University of Pune. We are also grateful to Dr T Shripathi and Mr M V Rama Rao (at IUC-DAEF, Indore) for helping us to obtain the XPS data and to Dr G K Dey, Dr D D Upadhyay and Dr S Banerjee for providing us with TEM facilities at BARC, Bombay.

References

[1] Eversole W G 1961 *US Patent Specification* 3030188
[2] Angus J C, Will H A and Stanko W S 1968 *J. Appl. Phys.* **39** 2915
[3] Spitsyn B V, Bouilov L L and Derjaguin B V 1981 *J. Cryst. Growth* **52** 219
[4] Angus J C and Hayman C C 1988 *Science* **241** 913 and references therein
[5] Yarbrough W A and Messier R 1990 *Science* **247** 688 and references therein

[6] Kelly M A, Olson D S, Kapoor S and Hagstrom S B 1992 *Appl. Phys. Lett.* **60** 2502
[7] Holcombe C E 1973 Calculated XRD data for polymorphic forms of carbon *Oak Ridge Y-12 Plant Report* Y-1887
[8] Verma A R and Krishna P 1966 *Polymorphism and Polytypism in Crystals* (New York: Wiley)
[9] Bundy F P and Kasper J S 1967 *J. Chem. Phys.* **46** 3437
[10] Spear K E, Phelps A W and White W B 1990 *J. Mater. Res.* **5** 2277
[11] Frenklach M, Kematick R, Huang D, Howard W, Spear K E, Phelps A W and Koba R 1989 *J. Appl. Phys.* **66** 395
[12] Sharma A K, Vispute R D, Joag D S, Ogale S B, Joag S D, Ayyub P, Multani M, Dey G K and Banerjee S 1993 *Mater. Lett.* **17** 42
[13] Andersen O K and Jepsen O 1984 *Phys. Rev. Lett.* **53** 2571
[14] Andersen O K, Jepsen O and Sob M 1987 *Electronic Band Structure and its Applications* ed M Yussouff (Berlin: Springer) p 1
[15] Andersen O K 1975 *Phys. Rev.* B **12** 3060
[16] Mackintosh A R and Andersen O K 1980 *Electrons at Fermi Surface* ed M Springford (New York: Cambridge University Press) p 187
[17] Salunke H G, Sharma A K, Das G P and Ayyub P 1995 *Phys. Rev.* B submitted
[18] Sharma A K, Adhi K P, Joag D S, Ogale S B, Dey G K and Banerjee S 1995 *Phys. Rev.* B submitted
[19] von Barth U and Hedin L 1972 *J. Phys. C: Solid State Phys.* **5** 1629
[20] Lambrecht W R L and Andersen O K 1986 *Phys. Rev.* B **34** 2439
Andersen O K, Postnikov A V and Savrasov S Yu 1991 *Applications of Multiple Scattering Theory to Materials Science (MRS Proc. 253)* ed W H Butler, P H Dederichs, A Gonis and R L Weaver (Pittsburgh, PA: Materials Research Society)
[21] Belton D S and Schmieg S J 1989 *J. Appl. Phys.* **66** 4223; 1990 *J. Vac. Sci Technol* A **8** 2353
[22] Wang Y, Hoffman R W and Angus J C 1990 *J. Vac. Sci. Technol* A **8** 2226
[23] Wang Y, Chen H, Hoffman R W and Angus J C 1990 *J. Mater. Res.* **5** 2378
[24] Fadley C S 1978 *Electron Spectroscopy: Theory, Techniques and Applications* vol 2, ed C R Brundle and A D Baker (London: Academic) p 59
[25] Nelson A J, Benson D K, Tracy C E, Kazmerski L L and Wager J F 1989 *J. Vac. Sci. Technol.* A **7** 1350
[26] Pollak R A, Ley L, McFeely F R, Kowalczyk S P and Shirley D A 1974 *J. Electron Spectrosc. Relat. Phenom.* **3** 381
[27] McFeely F R, Kowalczyk S P, Ley L, Cavell R G, Pollak R A and Shirley D A 1974 *Phys. Rev.* B **9** 5268
[28] Yoshikawa M, Katagiri G, Ishitani A, Ono M and Matsumura K 1989 *Appl. Phys. Lett.* **55** 2608
[29] Lurie P G and Wilson J M 1977 *Surf. Sci.* **65** 476
[30] *International Tables for X-ray Crystallography* 1969 ed N F M Henry and K Lonsdale (Birmingham: Kynoch)